A Low Complexity SI Sequence Estimator For Pilot-Aided SLM-OFDM Systems

Saheed A. Adegbite*, Scott G. McMeekin, Brian G. Stewart

School of Engineering and Built Environment, Glasgow Caledonian University, G4 0BA, Glasgow, UK

Abstract

Selected mapping (SLM) is a well-known method for reducing peak-to-average power ratio (PAPR) in orthogonal frequency division multiplexing (OFDM) systems. However, as a consequence of implementing SLM, OFDM receivers often require estimation of some side information (SI) in order to achieve successful data recovery. Existing SI estimation schemes have very high computational complexities that put additional constraints on limited resources and increase system complexity. To address this problem, an alternative SLM approach that facilitates estimation of SI in the form of phase detection is presented. Simulations show that this modified SLM approach produces similar PAPR reduction performance when compared to conventional SLM. With no amplifier distortion and in the presence of non-linear power amplifier distortion, the proposed SI estimation approach achieves similar data recovery performance as both standard SLM-OFDM (with perfect SI estimation) and also when SI estimation is implemented through the use of an existing frequency-domain correlation (FDC) decision metric. In addition, the proposed method significantly reduces computational complexity compared with the FDC scheme and an ML estimation scheme.

Keywords: OFDM, PAPR reduction, selected mapping, side-information detection

*Corresponding author, Tel: +44 141 273 1225
Email address: saheed.adegbite@gcu.ac.uk, sa.adegbite@gmail.com (Saheed A. Adegbite)

1. Introduction

Orthogonal frequency division multiplexing (OFDM) is now the preferred layer-1 technology in various high speed communication system standards including 4G-Long Term Evolution (4G-LTE) because it offers high spectral efficiency, immunity to multipath fading and provides a means to achieve very high data rate transmission. These are all attractive attributes of any high speed communication system [1, 2]. However, OFDM has a characteristic high peak-to-average power ratio (PAPR) [2–4], which may increase power consumption, degrade system performance and put additional constraints on the design and implementation of Power Amplifiers (PAs), Digital-to-Analogue (D/A) and Analogue-to-Digital (A/D) converters [3]. In addition, high PAPR signal levels often drive a PA to operate in its non-linear region, causing signal distortion in the form of increased bit-error-rate (BER). In theory, non-linear PA distortion can be avoided using a PA with a large linear region i.e. large input back off (IBO). Unfortunately, this approach is difficult to achieve in practice and it often results in poor PA efficiency, which reduces battery life span of mobile terminals and increases design costs [4, 5]. Therefore, for practical purposes, low PAPR signals are desirable in OFDM systems.

An in-depth review of various PAPR reduction techniques has been presented in [6]. Amongst these, is the selected mapping (SLM) scheme. SLM [7] is a well established method for reducing PAPR in OFDM. SLM creates alternative copies of the same OFDM signal by using a number of phase rotation sequences to modify phases of individual OFDM subcarriers within the original OFDM signal, then selecting and transmitting the time-domain signal that has the lowest PAPR value. Unfortunately, SLM introduces additional constraints in that it requires transmission and detection of some side information (SI), which contains vital information on how the transmitted OFDM signal was constructed at the transmitter. The transmission of SI reduces data throughput and the need for SI detection increases the receiver's computational requirements.

In pilot-aided OFDM systems, some SI estimation techniques that require no SI trans-

mission are discussed in [8] and [9]. Assuming all possible SLM phase rotation sequence vectors are known at the receiver, SI estimation is achieved in [8] using pilot-assisted Maximum Likelihood (PAML) and in [9] based on frequency-domain correlation (FDC) decision metrics. However, computational complexities associated with these schemes are high and are proportional to the number of alternative SLM phase rotation sequence vectors, U. These are unattractive when a larger value of U is used to improve the PAPR reduction performance. Also, since these pilot-assisted SI estimation schemes require the re-construction or storage of all U phase rotation sequence vectors at the receiver, there is a considerable level of system overhead associated with the implementation of both PAML and FDC SI estimation schemes.

To further reduce the computational complexity associated with SI estimation in pilot-assisted SLM-OFDM systems, this paper presents a pilot-assisted SI estimation method, which requires no SI transmission at the transmitter and no reconstruction of all candidate SLM phase rotation sequences at the receiver. The proposed method is also based on an extension of the work carried out in [10]. The proposed scheme in this paper differs from the work studied in [10] in that it uses a different SI estimation criterion based on a hard decision rule while the method in [10] applied a Maximum Likelihood (ML) detection criterion. For comparisons with the proposed method, the FDC based SI estimation scheme, presented in [9] is selected because it is based on the use of conventional SLM sequences and also gives slightly improved PAPR reduction performance over [8]. Simulations show that the modified SLM presented in this paper produces nearly similar PAPR reduction performance as conventional SLM. In addition, the proposed method achieves similar data recovery performance compared with existing SI estimation scheme presented in [9] and also when perfect knowledge of SI was assumed, with and without the presence of non-linear PA distortions.

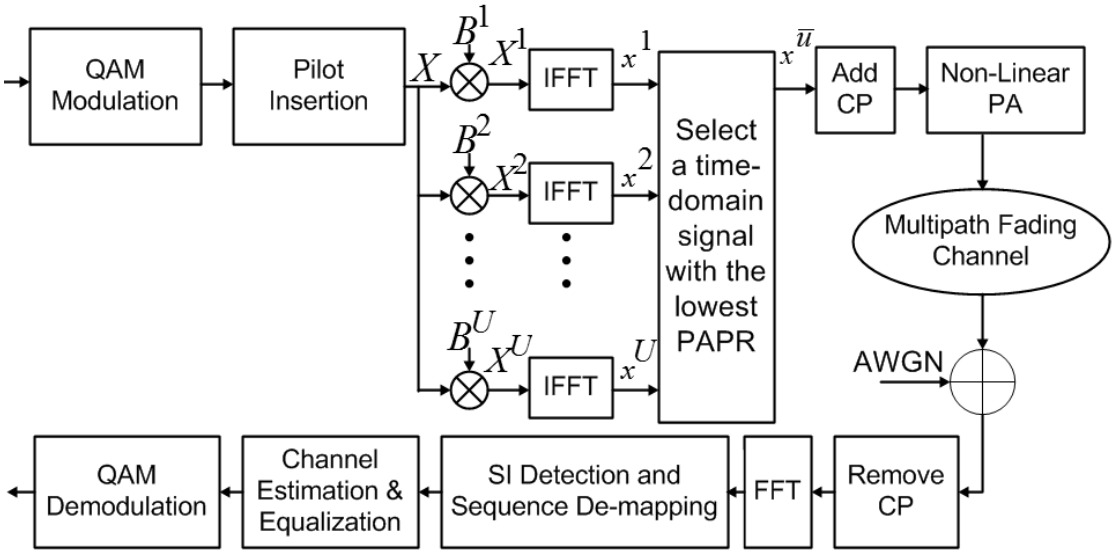

Fig. 1: SLM in pilot-aided OFDM i.e. SLM-OFDM

2. Conventional SLM-OFDM System and FDC Scheme

This section gives an overview of the conventional SLM method of reducing PAPR and SI estimation based on the FDC scheme studied in [9]. Fig. 1 shows a block diagram representation of a pilot-assisted SLM-OFDM system.

Conventional Pilot-assisted SLM-OFDM

Consider a pilot-aided OFDM symbol block $\boldsymbol{X}$ of length N_v, which consists of N_p pilot $\boldsymbol{X_p}$, and N_d data $\boldsymbol{X_d}$ symbols. For $0 \leq k \leq N_v - 1$ where k is a subarrier index, each subcarrier symbol denoted by $X[k]$ in $\boldsymbol{X}$ is mapped to a subcarrier index k through

$$\begin{aligned} X[k] &= X[mL + l], \qquad 0 \leq m \leq N_p - 1 \\ &= \begin{cases} X_p[mL], & l = 0 \\ X_d[mL + l], & \text{otherwise} \end{cases} \end{aligned} \tag{1}$$

where $N_v = N_d + N_p$, L represents the pilot spacing i.e. the number of subcarriers between two successive pilot symbols, l and m are arbitrary indices.

Using phase rotation sequence vectors denoted by $\boldsymbol{B^u}$ for $0 \leq u \leq U-1$, U alternative OFDM signals are constructed through SLM. One of the modified OFDM signals, denoted by $\boldsymbol{x^{\bar{u}}}$, will have the lowest PAPR value. Thus, the selected and transmitted signal $\boldsymbol{x^{\bar{u}}}$ is therefore given by

$$\begin{aligned} \boldsymbol{x^{\bar{u}}} &= IFFT\{\boldsymbol{B^{\bar{u}}} \cdot \boldsymbol{X}\} \\ &= \frac{1}{\sqrt{N}} \sum_{k=0}^{N_v-1} \left(B^{\bar{u}}[k] \cdot X[k]\right) \exp(-j2\pi nk/N) \end{aligned} \tag{2}$$

where $0 \leq n \leq N-1$.

The value of $\bar{u}$ is obtained from

$$\bar{u} = \underset{u \in 0,1, \ \ldots \ U-1}{\arg \min} \frac{\max\{|\boldsymbol{x^u}|^2\}}{\mathbb{E}\{|\boldsymbol{x^u}|^2\}}, \text{ where } \boldsymbol{x^u} = IFFT\{\boldsymbol{B^u} \cdot \boldsymbol{X}\} \tag{3}$$

where $\mathbb{E}\{\cdot\}$ is the expectation function for evaluating the mean power of signal $\boldsymbol{x^u}$.

The value of $\bar{u}$ must be known at the receiver in order to achieve successful data recovery since it contains the critical information on how $\boldsymbol{x^{\bar{u}}}$ was formed. The value of $\bar{u}$ or $\boldsymbol{B^{\bar{u}}}$ is commonly referred to as SI.

After transmission over a fading channel with frequency response $\boldsymbol{H}$, the received OFDM symbol $\bar{\boldsymbol{Y}}$ can be expressed as

$$\bar{\boldsymbol{Y}} = \boldsymbol{H}\boldsymbol{X^{\bar{u}}} + \boldsymbol{V}, \text{ where } \boldsymbol{X^{\bar{u}}} = \boldsymbol{X} \cdot \boldsymbol{B^{\bar{u}}} \tag{4}$$

where $\boldsymbol{V}$ represents complex-valued additive white Gaussian noise (AWGN) sequences. Similar to $\boldsymbol{X}$ in (1), data components of $\bar{\boldsymbol{Y}}$, $\boldsymbol{H}$ and $\boldsymbol{V}$ can be denoted by $\bar{\boldsymbol{Y}}_{\boldsymbol{d}}$, $\boldsymbol{H_d}$ and $\boldsymbol{V_d}$ respectively and their pilot components as $\bar{\boldsymbol{Y}}_{\boldsymbol{p}}$, $\boldsymbol{H_p}$ and $\boldsymbol{V_p}$ respectively. Since the SI is unknown at the receiver, it must be estimated.

FDC SI Estimation

Let $\hat{u}$ represent an estimate of the SI. Using the FDC based SI estimation studied in [9], $\hat{u}$ is obtained from

$$\hat{u} = \underset{u \in 0,1, \ldots U-1}{\arg\max} \; Re\{\boldsymbol{R}^u\} \tag{5}$$

where $\boldsymbol{R}^u$ is the FDC function, defined by

$$\boldsymbol{R}^u = \frac{1}{N_p - 1} \sum_{m=1}^{N_p-1} \hat{H}_p^u[m] \cdot \hat{H}_p^u[m-1]^*, \tag{6}$$

and

$$\hat{H}_p^u[m] = \frac{\bar{Y}_p[m] B_p^u[m]^*}{X_p[m]} \tag{7}$$

where * represents a complex conjugate operator.

In terms of computational complexity based on number of complex multiplications (CMs) and additions (CAs), the calculation of the FDC function $\boldsymbol{R}^u$ in (6) requires $U(N_p-1)$ CMs and $U(N_p-2)$ CAs while the computation of $\hat{H}_p^u[m]$ in (7) requires UN_p CMs. In total, the FDC based SI estimation scheme requires $U(2N_p-1)$ CMs and $U(N_p-2)$ CAs. It can be noted that these evaluations assume that $B_p^u[m] \in \pm 1$. In addition, since most implementations will involve real-valued operations, each complex-valued operation i.e. CMs and CAs are re-expressed in terms of real multiplications (RMs) and additions (RAs). From the definition in [9],

$$1 \text{ CM} \approxeq 4 \text{ RM} + 2 \text{ RA and } 1 \text{ CA} \approxeq 2 \text{ RA}. \tag{8}$$

Thus, the FDC scheme will require an estimated total number of $4(2UN_p - U)$ RMs and $6U(N_p-1)$ RAs.

Using the estimated SI value $\hat{u}$, SLM de-mapping is performed to remove the applied SLM phase rotation sequence value $B^{\bar{u}}[k]$ from each of the received subcarriers $\bar{Y}[k]$ through

an SLM de-mapping procedure, which gives

$$Y[k] = \bar{Y}[k]B^{\hat{u}}[k]^*. \tag{9}$$

Similarly, using the value of $\hat{u}$, the pilot sub-channel estimate $\hat{H}_p[m]$ is obtained from $\hat{H}_p^u[m]$ as

$$\hat{H}_p[m] = \hat{H}_p^{\hat{u}}[m]. \tag{10}$$

The next stage of data decoding involves finding an estimate of the received subcarrier symbol from

$$\hat{X}_d[k] = \min_{D[q]\in\mathbb{Q}} \left| Y_d[k] - \hat{H}_d[k]D[q] \right|^2 \tag{11}$$

where $\mathbb{Q}$ is the set of Q constellation points $D[q]$ of the chosen data modulation scheme for $0 \leq q \leq Q-1$, $\hat{X}_d[k] \in \mathbb{Q}$ is the estimated data symbol, and $\hat{H}_d[k]$ is an estimate of data sub-channel, obtained by linear interpolation between values of $\hat{H}_p[m]$.

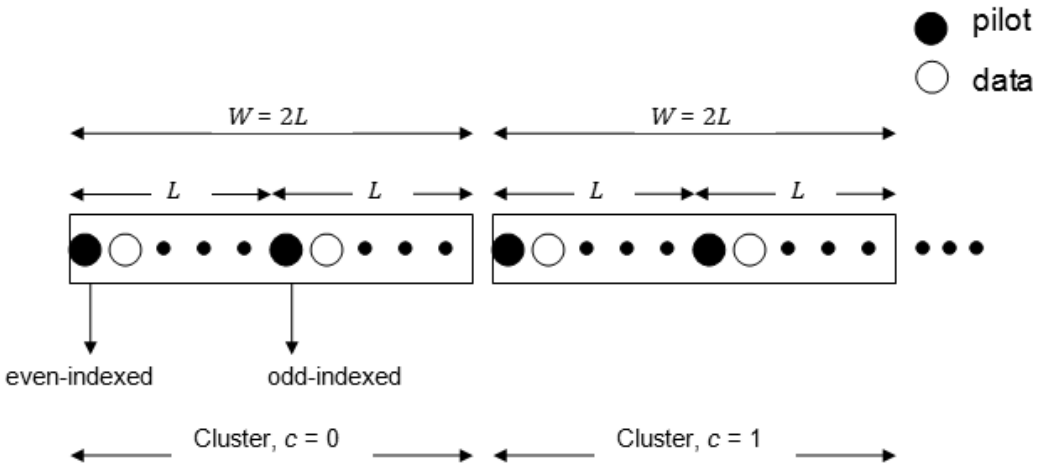

Fig. 2: Cluster representation showing data and pilots

3. Proposed Method

An alternative SI estimation method based on a binary phase detection approach is now proposed in an attempt to reduce the SI estimation computational complexity when compared with the methods in [9] and [10]. The proposed SI estimation method in this paper uses similar modified SLM method, which is referred to as clustered SLM (C-SLM), and is described in [10]. However, the proposed SI estimation is different compared with the approach in [10].

Similar to [10], the proposed method involves partitioning of OFDM symbol block $\boldsymbol{X}$ into $N_p/2$ consecutive clusters, each having two consecutive pilot symbols and $W-2$ data symbols where $W = 2L$.

Fig. 2 shows a block diagram representation of the considered clustering. For $0 \leq c < (N_p/2) - 1$, the cluster form of $X[k]$ can be represented by

$$\begin{aligned} X_c[w] = X[cW + w] = X[k],\ 0 \leq w \leq W-1 \\ = \begin{cases} X_c[w_e] = X_p[cW + w_e], & w_e = 0, w_e \in w \\ X_c[w_o] = X_p[cW + w_o], & w_o = L, w_o \in w \\ X_c[w_d] = X_d[cW + w_d], & \text{otherwise} \end{cases} \end{aligned} \tag{12}$$

where $w_d = 1,\ 2\ \ldots\ L-1,\ L+1\ \ldots\ W-1$, w_e and w_o represents w indices for every first and second pilot symbol in each cluster respectively. Henceforth, the first and second pilots in each cluster will be referred to as the 'even-indexed pilot' and 'odd-indexed pilot' respectively.

Similar to SLM, the C-SLM method produces alternative copies of the original OFDM symbol, then selects and transmits the one that has the lowest PAPR value. In contrast to SLM, which performs phase rotation on each of the subcarrier symbols (data and pilots) with different phase values, C-SLM phase rotates all data subcarrier symbol and the odd-index pilot in each cluster with a common phase value while the even-index pilot remains unchanged.

Let $\boldsymbol{J^u}$ represent C-SLM phase rotation sequences where $\boldsymbol{J^u} \in \pm 1$, elements of $\boldsymbol{J^u}$ are defined as

$$\begin{aligned} J_c^u[w] &= J^u[cW + w] = J^u[k] \\ &= \begin{cases} J_c^u[w_e] = 1 \\ J_c^u[w_o] = J_c^u[w_d] = J_c^u = \pm 1. \end{cases} \end{aligned} \tag{13}$$

Thus, application of $\boldsymbol{J^u}$ to $\boldsymbol{X}$ produces $\boldsymbol{X^u}$ as expressed through

$$\begin{aligned} X_c^u[w] &= X^u[cW + w] = X^u[k] \\ &= \begin{cases} X_c^u[w_e] = X_c[w_e] \\ X_c^u[w_o] = X_c[w_o] J_c^u \\ X_c^u[w_d] = X_c[w_d] J_c^u. \end{cases} \end{aligned} \tag{14}$$

The lowest PAPR signal $\boldsymbol{x^{\bar{u}}}$, obtained through C-SLM is given by

$$x_n^{\bar{u}} = \frac{1}{\sqrt{N}} \sum_{k=0}^{N_v - 1} X^{\bar{u}}[k] e^{\frac{j2\pi nk}{N}}, 0 \leq n \leq N-1 \tag{15}$$

where $\boldsymbol{X^{\bar{u}}} = \boldsymbol{X} \cdot \boldsymbol{J^{\bar{u}}}$ and $\boldsymbol{J^{\bar{u}}} = \boldsymbol{e^{j\alpha^{\bar{u}}}}$ denotes the optimum C-SLM sequence vector.

At the receiver, let $\boldsymbol{Z}$ represent the received OFDM sequences where $\boldsymbol{Z}$ is expressed by

$$\boldsymbol{Z} = \boldsymbol{H}\boldsymbol{X^{\bar{u}}} + \boldsymbol{V}. \tag{16}$$

Thus, each of the received subcarrier (in clustered form) $Z_c[w]$ is represented by

$$\begin{aligned} Z_c[w] &= H_c[w]X_c[w]J_c^{\bar{u}} + V_c[w], \\ &= \begin{cases} H_c[w_e]X_c[w_e] + V_c[w_e], & w = w_e, \\ H_c[w_o]X_c[w_o]J_c^{\bar{u}} + V_c[w_o], & w = w_o, \\ H_c[w_d]X_c[w_d]J_c^{\bar{u}} + V_c[w_d], & w = w_d. \end{cases} \end{aligned} \tag{17}$$

Unlike the FDC based SI estimation method previously described in (5), an estimate of the SI term $J_c^{\bar{u}}$ can also be achieved from the odd-indexed pilot since $J_c^{\bar{u}}[w_d] = J_c^{\bar{u}}[w_o] = J_c^{\bar{u}}$ [10].

First, an odd-indexed $\bar{H}_c[w_o]$ and an even-indexed $\hat{H}_c[w_e]$ terms are computed from

$$\begin{aligned} \hat{H}_c[w_e] &= \frac{Z_c[w_e]}{X_c[w_e]} = \frac{H_c[w_e]X_c[w_e] + V_c[w_e]}{X_c[w_e]} \\ &= H_c[w_e] + \frac{V_c[w_e]}{X_c[w_e]} \end{aligned} \tag{18a}$$

$$\begin{aligned} \bar{H}_c[w_o] &= \frac{Z_c[w_o]}{X_c[w_o]} = \frac{H_c[w_o]X_c[w_o]J_c^{\bar{u}} + V_c[w_o]}{X_c[w_o]} \\ &= H_c[w_o]J_c^{\bar{u}} + \frac{V_c[w_o]}{X_c[w_o]}. \end{aligned} \tag{18b}$$

At high signal-to-noise ratio (SNR) where the effects of the additive noise terms are negligible, a simplified expression for $\bar{H}_c[w_o]$ becomes

$$\bar{H}_c[w_o] \approx H_c[w_o]J_c^{\bar{u}} \tag{19}$$

From (18a) and (18b), it can be seen that the term $\hat{H}_c[w_e]$ differs from $\bar{H}_c[w_o]$ because

$\hat{H}_c[w_e]$ has no associated phase rotation value (since $J_c^{\bar{u}}[w_e] = 1$, see (13)) while $\bar{H}_c[w_o]$ has an associated phase rotation term $J_c^{\bar{u}}$. Therefore, $\hat{H}_c[w_e]$ represent the even-indexed pilot sub-channel estimate while $\bar{H}_c[w_o]$ represent an odd-indexed channel term.

It can be seen from the expression in (19) that an estimate of the SI term $J_c^{\bar{u}}$ can be obtained from $\bar{H}_c[w_o]$. However, since $\bar{H}_c[w_o]$ has an associated channel term $H_c[w_o]$, some form of channel cancellation is required to mitigate the channel fading effects. To achieve this, a 'normalised' (with respect to $\hat{H}_c[w_e]$) complex-valued term R_c is first obtained through

$$\begin{aligned} R_c &= \bar{H}_c[w_o] \Big/ \hat{H}_c[w_e] \\ &= \frac{H_c[w_o]J_c^{\bar{u}} + \frac{V_c[w_o]}{X_c[w_o]}}{H_c[w_e] + \frac{V_c[w_e]}{X_c[w_e]}}. \end{aligned} \tag{20}$$

By omitting the additive noise terms for simplicity, R_c can be re-expressed as

$$R_c \approx \frac{H_c[w_o]J_c^{\bar{u}}}{H_c[w_e]}. \tag{21}$$

By letting $\bar{\alpha}_c$ represent the phase component of R_c, a polar coordinate representation of R_c is given as

$$R_c = |R_c| \exp(j\bar{\alpha}_c). \tag{22}$$

From the expression in (21), it can be noted that by assuming a slow channel fading condition where $H_c[w_o] \approx H_c[w_e]$, an estimate $\hat{J}_c$ of the applied C-SLM sequence value $J_c^{\bar{u}}$ can be calculated from R_c.

The method in [10]

For each c index, let $\hat{J}_c$ denotes the estimate of $J_c^{\bar{u}}$ where $\hat{J}_c \in \pm 1$. Using the ML estimation approach described in [10], the SI estimate $\hat{J}_c$ is computed from

$$\hat{J}_c = \min_{\lambda_i \in \pm 1} \Big| \exp(j\bar{\alpha}_c) - \lambda_i \Big|^2 \tag{23}$$

where λ_i is an arbitrary variable used to determine whether $\hat{J}_c$ is $+1$ or -1 [10]. It can be seen that the implementation of (23) requires a total of N_p $|\cdot|^2$ operations and N_p CAs. However, the need for several $|\cdot|^2$ computations can increase the computational complexity of the method in [10].

An alternative SI estimation method is now proposed in an attempt to further reduce the computational complexity of computing $\hat{J}_c$. The proposed method is based on a hard decision criterion and is now described.

Proposed: Hard Decision Estimation

Since $J_c^{\bar{u}} \in \pm 1$, then its estimate $\hat{J}_c \in \pm 1$. Let $\hat{J}_c = \exp(j\hat{\alpha}_c)$ where the value of $\hat{\alpha}_c$ is either 0 or π. Unlike the ML method, $\hat{J}_c$ is indirectly determined from an estimate of the phase term $\hat{\alpha}_c$.

In the proposed method, an estimate of the phase term $\hat{\alpha}_c$ is calculated from a hard decision criterion given by

$$\hat{\alpha}_c = \begin{cases} 0, & \text{if } |\bar{\alpha}_c| \leq \pi/2 \\ \pi, & \text{otherwise} \end{cases} \tag{24}$$

where $\bar{\alpha}_c$ is the phase component of R_c as previously defined in (22). Note that since $\bar{\alpha}_c$ is a real-valued number, then the computational complexity of obtaining an absolute value of $\bar{\alpha}_c$ in (24) is negligible and is ignored.

From the expressions in (23) and (24), it can be noted that both methods (ML scheme and the proposed method) differ in their estimation of $\hat{J}_c$. It can also be seen that both methods require the computation of $\hat{H}_c[w_e]$ in (18a), $\bar{H}_c[w_o]$ in (18b), R_c in(20) and $\bar{\alpha}_c$ from R_c. The phase $\bar{\alpha}_c$ of a complex-valued variable (like R_c) can be evaluated through the use of the well-known Taylors series expansion described in [11, ch. 16]. It is estimated that using the Taylors expansion, $5N_p$ RMs and $2N_p$ RAs are required to evaluate the phase term $\bar{\alpha}_c$ from R_c (see the Appendix). Table 1 shows the computational complexity

Table 1: Computational complexity of computing $\hat{H}_c[w_e]$, $\bar{H}_c[w_o]$, $\bar{\alpha}_c$, and R_c

Variables	**Computational Complexity**
$\hat{H}_c[w_e]$ in (18a)	$N_p/2$ CMs $\equiv 2N_p$ RMs + N_p RAs
$\bar{H}_c[w_o]$ in (18b)	$N_p/2$ CMs $\equiv 2N_p$ RMs + N_p RAs
R_c in (20)	$N_p/2$ CMs $\equiv 2N_p$ RMs + N_p RAs
$\bar{\alpha}_c$ from R_c	$5N_p$ RMs + $2N_p$ RAs

of computing $\hat{H}_c[w_e]$, $\bar{H}_c[w_o]$, $\bar{\alpha}_c$ and R_c. As before, these evaluations (in Table 1) are re-expressed in terms of RAs and RMs computations using (8). Using the Taylors expansion method, computing the magnitude $|\cdot|$ of a complex-valued number requires 19 RMs and 8 RAs (see Appendix). Hence, computing N_p $|\cdot|^2$ operations in (23) requires $20N_p$ RMs + $8N_p$ RAs. Note that an additional RM operation is required to compute $|\cdot|^2$ compared with $|\cdot|$. Hence, the combined computational complexity of computing $\hat{H}_c[w_e]$, $\bar{H}_c[w_o]$, $\bar{\alpha}_c$ and R_c is $11N_p$ RMs + $5N_p$ RAs.

Using $\hat{J}_c$, data sub-channel estimates $\hat{H}_c[w_d]$ are obtained by linear interpolation between values of $\hat{H}_c[w_e]$ and $\hat{H}_c[w_o]$ where

$$\hat{H}_c[w_o] = \bar{H}_c[w_o]\hat{J}_c^*. \tag{25}$$

Using the channel estimates $\hat{H}_c[w_d]$ and $\hat{H}_c[w_o]$, channel equalization is achieved through

$$\begin{aligned}\hat{Y}_c[w_d] &= \frac{Z_c[w_d]}{\bar{H}_c[w_o]} \times \frac{\hat{H}_c[w_o]}{\hat{H}_c[w_d]} \\ &= \frac{H_c[w_d]X_c[w_d]J_c^{\bar{u}}}{H_c[w_o]J_c^{\bar{u}}} \times \frac{\hat{H}_c[w_o]}{\hat{H}_c[w_d]} \\ &= \frac{H_c[w_d]X_c[w_d]}{H_c[w_o]} \times \frac{\hat{H}_c[w_o]}{\hat{H}_c[w_d]}. \end{aligned} \tag{26}$$

In a similar to (11), the final data decoding stage determines an estimate of the nearest constellation point to $\hat{Y}_c[w_d]$.

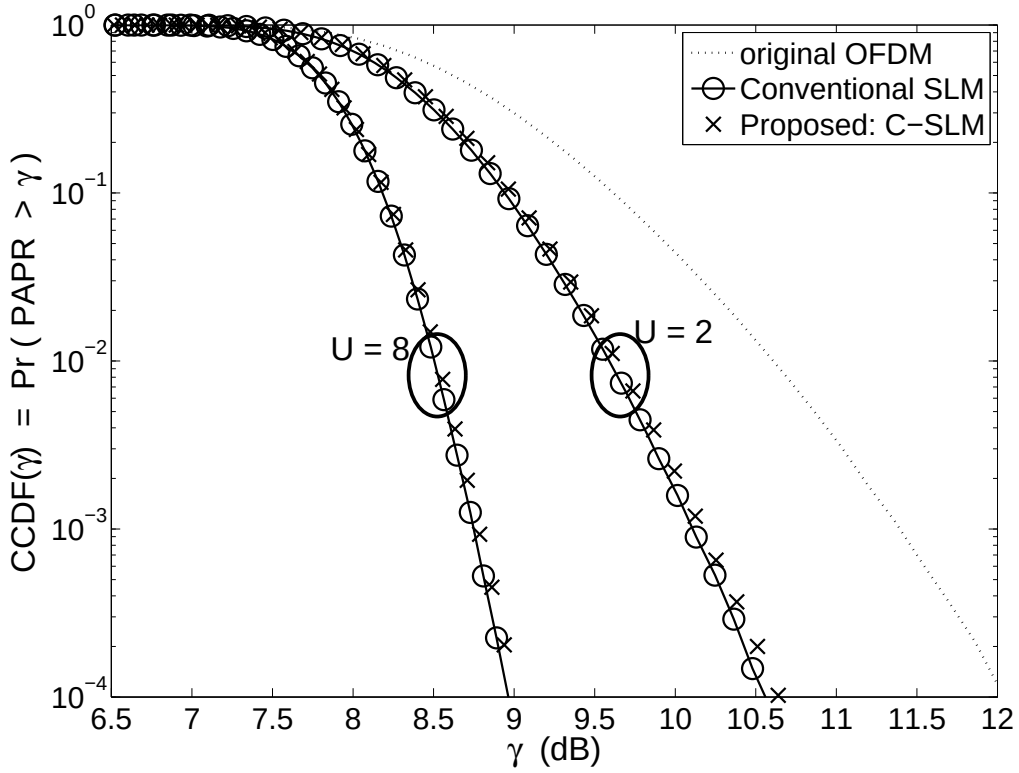

Fig. 3: Comparisons of CCDF curves

4. Simulation Results and Comparisons of Computational Complexity

This section presents comparisons of computational complexity of considered methods and discusses the Matlab simulation results on PAPR reduction and BER performance.

4.1. Simulation Results

With values of [N_p and L] set to [100 and 6] respectively, simulations consider OFDM transmission over three different channel models namely: (1) the extended pedestrian channel (EPA), defined in [12]; (2) 6-tap COST-207 rural-area channel (RA6), defined in [13] and (3) the 3GPP rural-area channel (3gppRA), defined in [14]. As defined for LTE systems, pilots are obtained from Gold codes sequences, OFDM subcarrier spacing is 15 KHz, guard interval is 5.21 μs and sampling frequency is set to 15.36 MHz (when $N = 1024$ and $N_v = 600$). Data symbols are obtained using a 64-QAM modulation scheme. SLM is performed using chaotic-binary sequences studied in [15] and PAPR reduction performance is measured by evaluating the well known complementary cumulative distribution function (CCDF). The CCDF gives the probability that a calculated PAPR of an OFDM signal exceeds a certain threshold denoted by γ. Thus, the CCDF of γ is defined as

$$\text{CCDF}\{\gamma\} = Prob(PAPR \geq \gamma). \tag{27}$$

Fig. 3 shows comparisons of CCDF curves of the OFDM signal before PAPR reduction (labelled as 'original OFDM'), with PAPR reduction using conventional SLM and the proposed C-SLM method for U set to 2 and 8. Results in Fig. 3 show that the proposed method produces nearly similar PAPR reduction performance as conventional SLM for each value of U.

With U set to 8, BER is evaluated by considering some pre-defined levels of PA linearity

using the IBO parameter. The IBO of a PA is defined as

$$\text{IBO (dB)} = 10\log_{10}\left(\frac{P_{sat}}{P_{avg}}\right) \tag{28}$$

where P_{sat} and P_{avg} respectively denote PA input saturation power and mean power of the input signal. In this paper, the amplitude modulation (AM) effects of PA is modelled using the well known Rapp's model [16]. Simulations consider a solid state PA (SSPA), commonly used in mobile communications systems [17]. The output AM/AM conversion of a SSPA, with unity gain, is described by Rapp's model through

$$y(t) = \frac{x(t)}{\left[1 + \left(\frac{|x(t)|}{A_{sat}}\right)^{2\rho}\right]^{1/2\rho}} \tag{29}$$

where $x(t)$ represents the input signal into the SSPA, $y(t)$ is the output signal from the SSPA, A_{sat} is the SSPA output saturation magnitude and ρ is the smoothing factor which controls the PA's transition from linear to saturation region i.e. the higher the value of ρ, the sharper the transition from linear to non-linear operating region of the SSPA. For accurate modelling of an SSPA, ρ is set to 3 [18, ch. 2].

The data recovery performance of the proposed method is compared with that of a standard SLM-OFDM (when perfect SI knowledge is assumed) and with SI estimation based on the FDC scheme for IBO values: ∞ dB, 2 dB, and 6 dB. Note that the case when IBO $= \infty$ dB represent an SLM-OFDM system with no non-linear PA distortion i.e. linear PA.

Figs. 4 to 6 compare BER curves between the proposed method, standard SLM-OFDM (which assumes perfect SI estimation) and the FDC method over EPA, RA6 and 3gppRA channel fading conditions respectively. Results show that for each of the considered channel

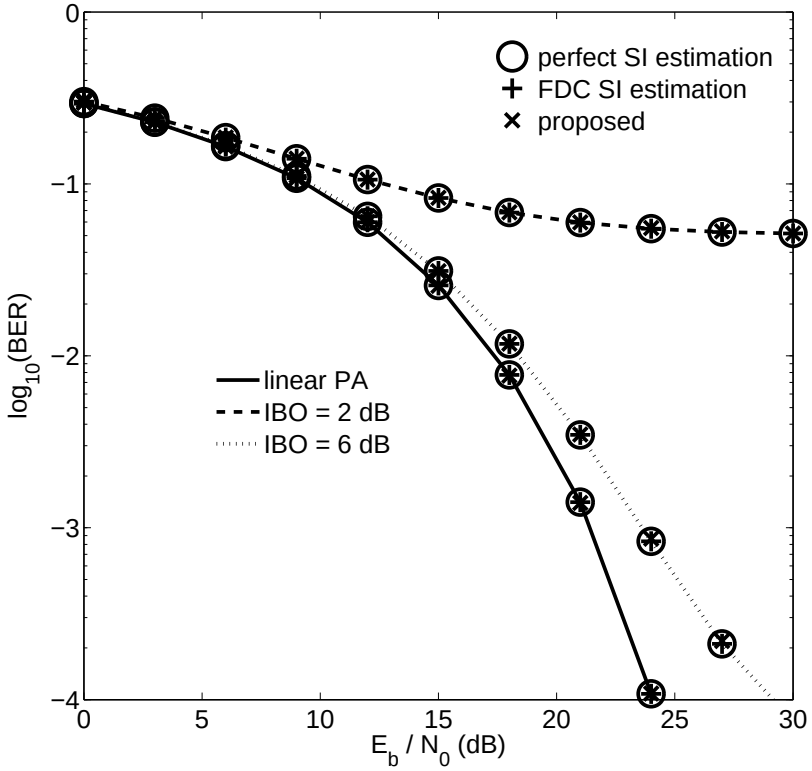

Fig. 4: BER comparisons: EPA fading channel

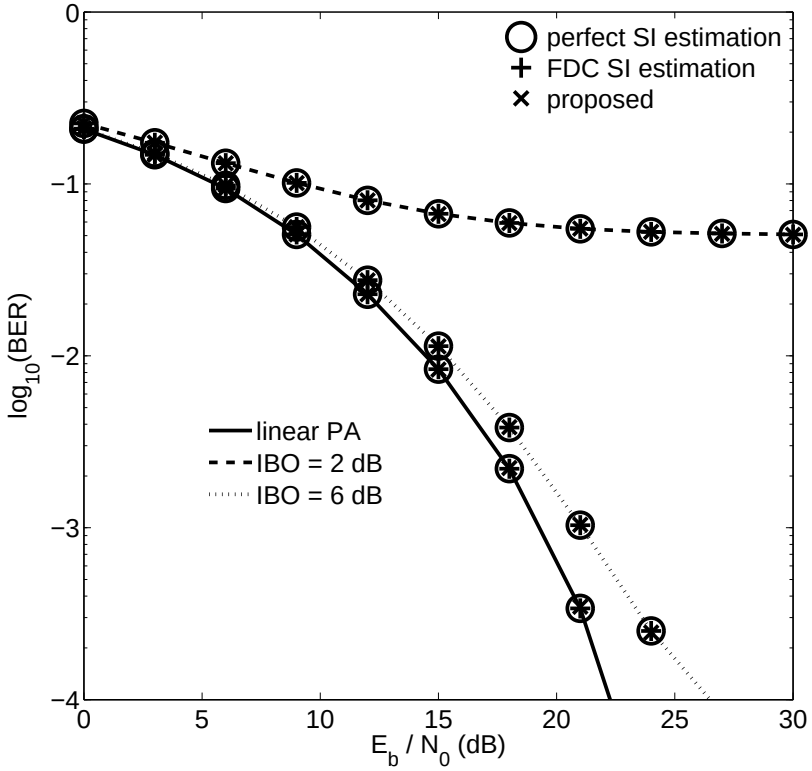

Fig. 5: BER comparisons: RA6 fading channel

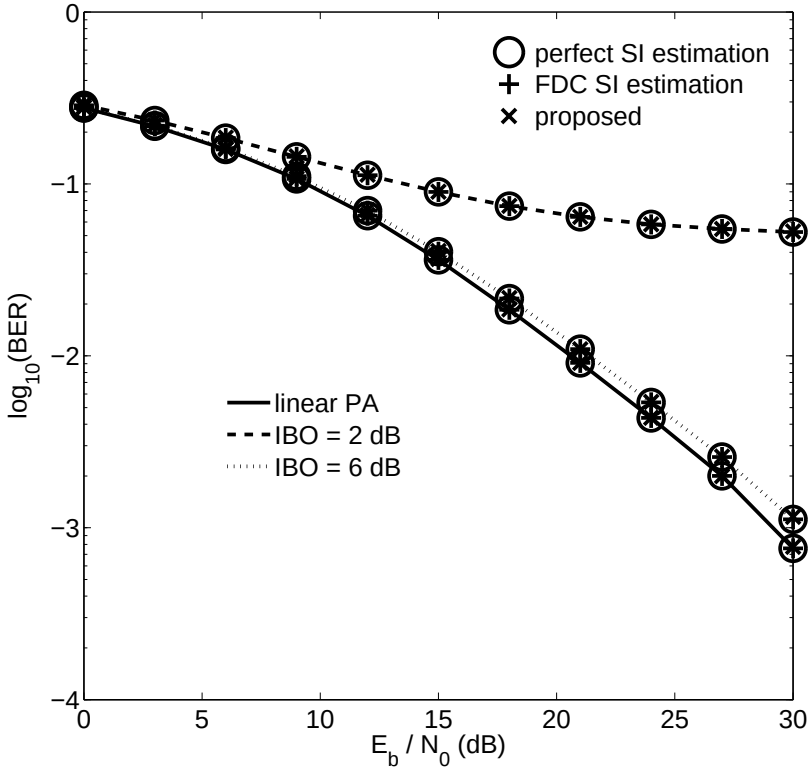

Fig. 6: BER comparisons: 3gppRA fading channel

environments and IBO levels, the proposed method produces the same BER performance as both the FDC based SI estimation scheme and standard SLM-OFDM, which assumes perfect knowledge of SI. This is partly because of the inherent phase cancellation (SLM de-mapping) within the proposed method, and also because of the slow fading channel conditions.

It can be noted the BER performance of the ML estimation method described in [10] is not presented to avoid duplicity of previous results in [10]. The key advantage of the proposed method over the FDC based SI estimation scheme and the ML method is now demonstrated through the comparison of their computational complexity.

4.2. Computational Complexity

From the previous descriptions in Table 1, Table 2 shows summary of the computational requirements of computing expressions in (23) and (24) for the ML estimation method in [10] and the proposed method respectively. From Table 2, it can be seen that the proposed scheme requires a total of $11N_p$ RM and $5N_p$ RA computations while the ML estimation method in [10] requires $31N_p$ RMs and $15N_p$ RAs. Note that these evaluations ignores the complexity of real-valued compare operations because it is negligible relative to the complexity of RMs and RAs. Table 3 shows comparisons of the number of RM and RA operations required by the FDC, the ML estimation method in [10] and the proposed method.

It can be noted (in Table 3) that the computational complexity of both the proposed method and the method in [10] is independent of the value of U. In addition, unlike the FDC scheme, both the ML estimation approach and the proposed method require no knowledge of all candidate SLM sequences during data decoding. Therefore, it is expected that the proposed method has a significant computational advantage (over the FDC scheme) as the value of U is increased.

Using Table 3, the computational complexity advantage of the proposed method is numerically evaluated using the well known Computational Complexity Reduction Ratio (CCRR) metric relative to the FDC scheme and the ML estimation method (based on RAs

Table 2: Computation requirements of the ML estimation method in [10] and the proposed SI estimation method

ML method [10]	**Proposed**
$\hat{J}_c$ is directly computed from (23)	$\hat{J}_c$ is computed as $\exp(j\hat{\alpha}_c)$ where $\hat{\alpha}_c$ is derived from (24)
Complexity of computing $\hat{H}_c[w_e]$, $\bar{H}_c[w_o]$, $\bar{\alpha}_c$ and R_c is $11N_p$ RMs + $5N_p$ RAs	Same as the ML method.
The expression in (23) requires N_p $\lvert\cdot\rvert^2$ and N_p CAs. Note that N_p CAs $\equiv$ $2N_p$ RAs and each $\lvert\cdot\rvert^2$ requires $20N_p$ RMs plus $8N_p$ RAs.	To compute $\hat{\alpha}_c$, $N_p/2$ real-valued compare operations are required.
Total: $31N_p$ RMs + $15N_p$ RAs	Total: $11N_p$ RMs + $5N_p$ RAs

and RMs). The CCRR is defined as [9]

Table 3: Comparisons of computational complexity in terms of RMs and RAs

Computational Complexity	**FDC**	**Method in [10]**	**Proposed**
RMs	$4(2UN_p - U)$	$31N_p$	$11N_p$
RAs	$6U(N_p - 1)$	$15N_p$	$5N_p$

$$\text{CCRR} = \left(1 - \frac{\text{complexity of the proposed method}}{\text{complexity of other scheme}}\right) \times 100\%. \tag{30}$$

The CCRR value represents the amount (expressed as a %) of reduction in computational complexity offered by the proposed method relative to either the FDC scheme or the ML approach [19]. Table 4 shows comparisons of estimated CCRR values for RMs and RAs when U is set to: 4, 8 and 16. High CCRR values for the proposed method as highlighted in Table 4 suggest that the proposed method requires significantly reduced computational complexity compared with the existing FDC scheme in [9] and the ML method in [10]. As expected, it can be seen that the computational complexity of the ML approach is independent on the value of U.

5. Conclusions

An alternative SI estimation technique is proposed for an SLM-OFDM receiver. The proposed method used a modified SLM scheme known as C-SLM to reduce PAPR and performed SI estimation through the use of a hard binary decision rule. In terms of PAPR reduction, the C-SLM method offered nearly similar PAPR reduction capability to conventional SLM. Also, unlike the FDC scheme, the proposed SI estimation method obtains SI

Table 4: CCRR of the proposed method relative to both the FDC scheme and the ML method

Parameters	Operations	FDC scheme	ML method
$U = 4$	**RM**	77%	64%
	RA	84%	66%
$U = 8$	**RM**	88%	64%
	RA	92%	66%
$U = 16$	**RM**	94%	64%
	RA	96%	66%

estimates without the knowledge of all possible phase rotation sequences and produced similar data recovery performance to both standard SLM-OFDM (with perfect knowledge of SI) and the FDC based SI estimation scheme. The proposed method is an attractive choice over other methods because it required significantly reduced computational complexity.

Appendix

Computing Amplitude and Phase of a Complex Number

For a complex number $\mathcal{C}$, let $|\mathcal{C}|$ and θ respectively be the magnitude and phase of $\mathcal{C}$. The real and imaginary components of $\mathcal{C}$ is respectively represented by $\mathcal{C}_{\text{re}}$ and $\mathcal{C}_{\text{im}}$. Then, from Euler's formula, the complex number $\mathcal{C}$ is given by

$$\begin{aligned}\mathcal{C} &= \mathcal{C}_{\text{re}} \pm j\mathcal{C}_{\text{im}} = |\mathcal{C}| \exp(\pm j\theta) \\ &= |\mathcal{C}| \cos(\theta) \pm j|\mathcal{C}| \sin(\theta). \end{aligned} \tag{31}$$

Given $\mathcal{C}$, θ can be computed from

$$\theta = \tan^{-1}\left(\mathcal{C}_{\text{im}} \Big/ \mathcal{C}_{\text{re}}\right). \tag{32}$$

From the expression in (31), the magnitude $|\mathcal{C}|$ is obtained as

$$|\mathcal{C}| = \mathcal{C}_{\text{re}} \Big/ \cos(\theta) \quad \text{OR} \quad |\mathcal{C}| = \mathcal{C}_{\text{im}} \Big/ \sin(\theta). \tag{33}$$

Using numerical computational methods, the arctangent function $\tan^{-1}(x)$ in (32) is computed using Taylor series expansion described in [20]

$$\tan^{-1}(x) = x - \frac{x^3}{3} + \frac{x^5}{5} - \frac{x^7}{7} + \frac{x^9}{9} - \quad \ldots \tag{34}$$

Note that x is a real-valued number. Using a Matlab tool called taylortool, it was verified that the first 5 terms in a Taylor series approximation is sufficient to produce identical results as that from actual Matlab implementation of trigonometric functions.

Computational Complexity of Computing $\theta = tan^{-1}(x)$

To compute $\tan^{-1}(x)$ using the expression in (34), the x^2 term is first computed so as to enable the subsequent computation of x^3, x^5, x^7 and x^9 terms.

The computation of x^2 requires 1 real multiplication (RM), and the computation of x^3, x^5, x^7 and x^9 each require 1 RM according to the following:

$$\begin{aligned} x^3 &= x^2 \cdot x \,; \quad & x^5 &= x^3 \cdot x^2 \\ x^7 &= x^5 \cdot x^2 \,; \quad & x^9 &= x^7 \cdot x^2 \end{aligned} \tag{35}$$

Here, it is assumed that the computation of, for example, x^7 will use the results from the initial computation of x^5 and the pre-computed x^2. Similarly, the computation of x^9 will use initial results of x^7 and x^2.

The four divisions and additions in (34) require equivalent of 4 RMs and 4 real additions (RAs). Hence, a total number of 9 RMs and 4 RAs are required to compute $\tan^{-1}(x)$. Therefore, to compute the phase of a complex number, 10 RMs and 4 RAs operations are required (the additional RM is from the division in (32)).

Computational Complexity of Computing θ

= 10 RMs plus 4 RAs

Computational Complexity of Computing $|\mathcal{C}|$

From the expression in (33), the cosine function $\cos(\theta)$ can also be derived using the Taylor series expansion [20]

$$\cos(\theta) = 1 - \frac{\theta^2}{2!} + \frac{\theta^4}{4!} - \frac{\theta^6}{6!} + \frac{\theta^8}{8!} - \quad \ldots \tag{36}$$

Note that θ is also a real-valued number and the evaluations in (36) assume that the factorial of a number is pre-computed and known. Similar to the arctan function, the first 5 terms of Taylor series implementation of a cosine function is found to give a good approximation.

In a similar manner to $\tan^{-1}(x)$, computing $\cos(\theta)$ also requires 8 RMs and 4 RAs. Hence, to compute the magnitude $|\mathcal{C}|$ of a complex number, a total number of 19 RMs and 8 RAs is required. Note that the additional RM is from the division operation in (33).

Computational Complexity of Computing $|\mathcal{C}|$

= 19 RMs plus 8 RAs

References

[1] S. Adegbite, B. G. Stewart, S. G. McMeekin, Least Squares Interpolation Methods for LTE System Channel Estimation over Extended ITU Channels, International Journal of Information and Electronics Engineering 3 (4) (2013) 414–418.

[2] N. I. Miridakis, D. D. Vergados, A Survey on the Successive Interference Cancellation Performance for Single-Antenna and Multiple-Antenna OFDM Systems, Communications Surveys Tutorials, IEEE 15 (1) (2013) 312–335.

[3] T. Jiang, Y. Wu, An Overview: Peak-to-Average Power Ratio Reduction Techniques for OFDM Signals, Broadcasting, IEEE Transactions on 54 (2) (2008) 257–268.

[4] X. Li, L. J. Cimini, Effects of clipping and filtering on the performance of OFDM, Communications Letters, IEEE 2 (5) (1998) 131–133.

[5] G. Santella, F. Mazzenga, A hybrid analytical-simulation procedure for performance evaluation in M-QAM-OFDM schemes in presence of nonlinear distortions, Vehicular Technology, IEEE Transactions on 47 (1) (1998) 142–151.

[6] Y. Rahmatallah, S. Mohan, Peak-To-Average Power Ratio Reduction in OFDM Systems: A Survey And Taxonomy, Communications Surveys Tutorials, IEEE 15 (4) (2013) 1567–1592.

[7] R. W. Bauml, R. F. H. Fischer, J. B. Huber, Reducing the peak-to-average power ratio of multicarrier modulation by selected mapping, Electronics Letters 32 (22) (1996) 2056 –2057.

[8] J. Park, E. Hong, D. Har, Low Complexity Data Decoding for SLM-Based OFDM Systems without Side Information, Communications Letters, IEEE 15 (6) (2011) 611–613.

[9] E. Hong, H. Kim, K. Yang, D. Har, Pilot-Aided Side Information Detection in SLM-Based OFDM Systems, Wireless Communications, IEEE Transactions on 12 (7) (2013) 3140–3147.

[10] S. A. Adegbite, S. G. McMeekin, B. G. Stewart, Low-complexity data decoding using

binary phase detection in SLM-OFDM systems, Electronics Letters 50 (7) (2014) 560–562.

[11] J. Y. Stein, Digital Signal Processing: A Computer Science Perspective, A Wiley interscience publication, Wiley, 2000.

[12] 3GPP Technical Specification (TS) 36.101 v12.0.0, Evolved Universal Terrestrial Radio Access (E-UTRA); User Equipment (UE) Radio Transmission and Reception (Release 12) (July 2013).

[13] M. Failli, Digital land mobile radio communications COST 207.

[14] ETSI Technical Report (TR) 125.943 v11.0.0, Universal Mobile Telecommunications System (UMTS); Deployment aspects (Release 11) (Oct. 2012).

[15] C. Peng, X. Yue, D. Lilin, L. Shaoqian, Improved SLM for PAPR Reduction in OFDM System, in: Personal, Indoor and Mobile Radio Communications, 2007. PIMRC 2007. IEEE 18th International Symposium on, 2007, pp. 1–5.

[16] C. Rapp, Effects of HPA nonlinearity on a 4-DPSK/OFDM signal for a digital sound broadcasting system, in: Proc. 2nd European Conference on Satellite Communication, Liege, Belgium, 1991, pp. 179–184.

[17] Y. Guo, J. R. Cavallaro, A novel adaptive pre-distorter using LS estimation of SSPA non-linearity in mobile OFDM systems, in: Circuits and Systems, 2002. ISCAS 2002. IEEE International Symposium on, Vol. 3, 2002, pp. 453–456.

[18] L. Smaini, RF Analog Impairments Modeling for Communication Systems Simulation: Application to OFDM-based Transceivers, Wiley, 2012.

[19] S. A. Adegbite, S. McMeekin, B. G. Stewart, Performance of a New Joint PAPR Reduction and SI Estimation Technique for pilot-assisted SLM-OFDM Systems, in:

Communication Systems, Networks Digital Signal Processing (CSNDSP), 2014 9th IEEE/IET International Symposium on, 2014, pp. 308–313.

[20] J. Y. Stein, Digital Signal Processing: A Computer Science Perspective, Wiley, 2000, ch. 16.